

A molecular dynamics simulations study on the relations between dynamical heterogeneity, structural relaxation, and self-diffusion in viscous liquids

Patrick Henritzi, André Bormuth, Felix Klameth, and Michael Vogel

Citation: *The Journal of Chemical Physics* **143**, 164502 (2015); doi: 10.1063/1.4933208

View online: <http://dx.doi.org/10.1063/1.4933208>

View Table of Contents: <http://scitation.aip.org/content/aip/journal/jcp/143/16?ver=pdfcov>

Published by the **AIP Publishing**

Articles you may be interested in

[Dynamic asymmetry of self-diffusion in liquid ZnCl₂ under pressure: An ab initio molecular-dynamics study](#)
J. Chem. Phys. **138**, 134504 (2013); 10.1063/1.4798376

[A molecular dynamics examination of the relationship between self-diffusion and viscosity in liquid metals](#)
J. Chem. Phys. **136**, 214505 (2012); 10.1063/1.4723683

[Diffusion and viscosity of liquid tin: Green-Kubo relationship-based calculations from molecular dynamics simulations](#)
J. Chem. Phys. **136**, 094501 (2012); 10.1063/1.3687243

[Quantum diffusion in liquid water from ring polymer molecular dynamics](#)
J. Chem. Phys. **123**, 154504 (2005); 10.1063/1.2074967

[Self-diffusion and Spatially Heterogeneous Dynamics in Supercooled Liquids Near T_g](#)
AIP Conf. Proc. **708**, 491 (2004); 10.1063/1.1764214



NEW Special Topic Sections

NOW ONLINE
Lithium Niobate Properties and Applications:
Reviews of Emerging Trends

AIP Applied Physics
Reviews

A molecular dynamics simulations study on the relations between dynamical heterogeneity, structural relaxation, and self-diffusion in viscous liquids

Patrick Henritzi, André Bormuth, Felix Klameth, and Michael Vogel

Institut für Festkörperphysik, Technische Universität Darmstadt, 64289 Darmstadt, Germany

(Received 20 July 2015; accepted 2 October 2015; published online 23 October 2015)

We perform molecular dynamics simulations for viscous liquids to study the relations between dynamical heterogeneity, structural (α) relaxation, and self-diffusion. For atomistic models of supercooled water, polymer melts, and an ionic liquid, we characterize the space-time characteristics of dynamical heterogeneity by the degree of deviations from Gaussian displacement statistics (α_2), the size of clusters comprising highly mobile particles (S_w), and the length of strings consisting of cooperatively moving particles (L_w). Comparison of our findings with previous simulation results for a large variety of viscous liquids, ranging from monoatomic liquids to silica melt, reveals a nearly universal decoupling between the time scales of maximum non-Gaussian parameter (τ_{α_2}) and the time constant of the α relaxation (τ_α) upon cooling, explicitly, $\tau_{\alpha_2} \propto \tau_\alpha^{3/4}$. Such uniform relation was not observed between the peak times of S_w or L_w and τ_α . On the other hand, the temperature-dependent time scale of maximum string length (τ_L) follows the inverse of the self-diffusion coefficient (D) for various systems at sufficiently low temperatures, i.e., $\tau_L \propto D^{-1}$. These observations are discussed in view of a breakdown of the Stokes-Einstein relation for the studied systems. It is found that the degree of deviation from this relation is correlated with the stretching of the α relaxation. © 2015 AIP Publishing LLC. [<http://dx.doi.org/10.1063/1.4933208>]

I. INTRODUCTION

The slowdown of molecular dynamics (MD) in liquids approaching a glass transition is of great importance in fundamental and applied sciences.^{1–4} When glass-forming liquids are cooled towards the glass transition temperature T_g , the structural (α) relaxation times increase by several orders of magnitude. For fragile glass formers, the temperature dependence of the structural relaxation deviates from an Arrhenius behavior and the correlation functions of this dynamical process differ from a single exponential. Likewise, when glass-forming liquids are exposed to elevated pressure, the α relaxation slows down in most cases, resulting in a pressure-dependent value of T_g .

MD simulations provide detailed insights into the structural relaxation of viscous liquids on time scales up to the microseconds regime,^{4–10} limited by the computing power. While first applications focused on simple model glass-formers, e.g., Lennard-Jones (LJ) mixtures or bead-spring polymers,^{11–17} recent improvements in computer performance paved the way for works on chemically realistic all-atom models of molecular systems, including polymer melts.^{8,9,18,19} Thus, MD simulations became an important tool to ascertain the initial slowdown of particle dynamics in liquids approaching a glass transition.

Experimental studies showed that the nonexponential α relaxation of viscous liquids is linked to the possibility to select particles that exhibit significantly higher or lower mobilities than an average particle.^{20–23} Simulation analyses yielded detailed insights into spatial correlations between particles of a given mobility. It was found that spatially heterogeneous dynamics (SHD) become a prominent feature of glass-forming

liquids upon cooling.^{11–19,24–28} Other approaches focused on the relation between structural relaxation and particle diffusion. Experimental^{29–35} and computational^{26–28,36–44} studies reported that the Stokes-Einstein relation (SER) breaks down in viscous liquids and some of these works proposed a fractional SER.

Starting with Hodgdon and Stillinger,⁴⁵ several authors considered the existence of SHD as the cause of the SER breakdown.^{3,23} Specifically, it was argued that structural relaxation is governed by slow particles, while self-diffusion is dominated by fast particles so that a broadening of the distribution of particle mobilities upon cooling results in such breakdown. However, the exact relation between the existence of SHD and the failure of the SER remains elusive. Frustration-limited domains⁴⁶ and dynamic facilitation models^{47,48} provided static and dynamic views, respectively. Also, this breakdown was explained based on the mosaic picture of the random first-order transition theory⁴⁹ or the increase of critical fluctuations of the mode-coupling theory.⁵⁰ Furthermore, this phenomenon was traced back to an onset of activated barrier hopping^{51,52} or rationalized within energy-landscape models.⁵³ On the other hand, it was proposed that it is not necessary to invoke SHD to elucidate the SER breakdown.^{54,55}

The capabilities of MD simulations were exploited to discriminate between various explanations for the failure of the SER. A relation to SHD received support from the observation of decoupling master curves in scaling approaches, which are based on the growth of dynamic clusters.³⁶ Also, SER violations were found to be sensitive to the size⁵⁶ and shape⁵⁷ of dynamically distinguishable regions. Some workers reported that the breakdown of the SER is due to fast particles, while slow particles obey this relation.^{39,40} By contrast, other workers

argued that neither fast nor slow particles obey the SER.^{26,38} MD work did not observe a relation between the fragility of the liquid and the degree of deviation from the SER,⁴² which is predicted by the dynamic facilitation model and the random first-order transition theory.^{48,49} Finally, simulation studies showed that the decoupling of relaxation time and diffusion coefficient sets in well above the critical temperature T_c of mode-coupling theory.^{36,40,42}

Here, MD simulations are performed for all-atom models of supercooled water, polymer melts, and an ionic liquid (IL). We investigate the structural relaxation and the self-diffusion of these glass formers in broad ranges of temperature and pressure and we consider polymer chains of various lengths. In addition to the present results, our analyses include the literature data from simulation works on glass-forming liquids. Observing various manifestations of SHD, the time scale of dynamical heterogeneity is compared with that of the structural relaxation and diffusive dynamics. Moreover, the extent of SHD is related to the degree of the breakdown of SER, as characterized by a fractional Stokes-Einstein exponent.

II. METHODS

A. Simulation details

MD simulation studies are performed for supercooled water, polyethylene oxide (PEO), polypropylene oxide (PPO), polybutadiene (PBD), and for an IL comprised of 1-*n*-butyl-3-methylimidazolium cations and hexafluorophosphate anions. With the exception of PBD, the used models are described by all-atom force fields. The bonded interactions comprise contributions from bond stretching, bond bending, and torsional motion. The nonbonded interactions include Coulomb interactions, van der Waals attractions, and Pauli repulsions, which are modeled by LJ or Buckingham potentials, depending on the system.

Details of the MD simulations for the PEO and PPO systems, which use force-field parameters from quantum chemical calculations,^{58,59} can be found in our previous studies.^{18,19,60} The PBD model is a united-atom model exhibiting 40% *cis*, 50% *trans*, and 10% 1,2 vinyl units, which are randomly distributed along the chain.⁶¹ To specify the polymer systems, we use the names together with an index describing the chain length, e.g., PPO_{*n*} refers to polypropylene oxide with *n* monomeric units. We show results for PEO₁₂, PBD₁₀₀, and PPO with various chain lengths *n* = 2–100. The water system was specified in two prior works.^{62,63} It uses the SPC/E water model.⁶⁴ The IL consists of 256 ion pairs. The force-field parameters can be found in the literature.^{65–67} All these models proved well suited to reproduce many thermodynamic, structural, and dynamical properties of the corresponding viscous liquids.

The GROMACS software package^{68–72} was utilized for the MD simulations. The particle-mesh Ewald method⁷³ was applied to calculate the Coulomb interactions. The Nosé-Hoover thermostat^{74,75} and the Parrinello-Rahman barostat⁷⁶ were employed to set the temperature (*T*) and pressure (*P*), respectively. Time steps of 1–2 fs were used. Prior to data acquisition, equilibration runs were performed in the NPT ensemble to adjust the volume (*V*) of the cubic simulation

boxes for set values of *T*, *P*, and the number of atoms *N*. We ensured that the equilibration times always exceeded the time scale of α relaxation. The production runs were conducted in the NVT ensemble. If not stated otherwise, the data correspond to ambient pressure. For PPO₄, additional simulations were performed at elevated pressure *P* = 1, 6, and 10 kbar.

B. Characterization of structural relaxation and self-diffusion

To investigate the diffusive motion, we compute the mean-square displacement (MSD) from the particle translations during a time interval *t*, $\mathbf{r}_i(t_0 + t) - \mathbf{r}_i(t_0)$, so that the self-diffusion coefficient *D* can be obtained from the long-time behavior according to

$$\langle [\mathbf{r}_i(t_0 + t) - \mathbf{r}_i(t_0)]^2 \rangle = 6Dt. \quad (1)$$

In studies of polymeric systems, it is particularly important to ensure that the long-time limit is reached since polymer dynamics, e.g., Rouse dynamics delays the onset of the diffusive regime.⁷⁷ Throughout this contribution, the angular brackets $\langle \dots \rangle$ denote an ergodic average over all specified atoms and available time origins *t*₀. To analyze the α relaxation, we calculate the incoherent scattering function (ISF),

$$F_s(q, t) = \langle \cos \{ \mathbf{q} [\mathbf{r}_i(t_0 + t) - \mathbf{r}_i(t_0)] \} \rangle. \quad (2)$$

It probes the particle displacements on a length scale determined by the modulus of the scattering vector, $q = |\mathbf{q}|$. To ensure observation of structural relaxation, we use, unless otherwise stated, scattering vectors corresponding to typical intermolecular distances. From the ISF, we obtain a time constant of the α relaxation, τ_α , according to $F_s(q, t = \tau_\alpha) = 1/e$.

For the analyses of the MSD and ISF and for the characterization of SHD, as described below, we use the time-dependent positions of the oxygen atoms in the cases of SPC/E, PEO, and PPO and of the united (CH) carbon atoms in the case of PBD. For the IL, we distinguish between the phosphorus atoms in the anions (IL an) and the carbon atoms bonded to two nitrogen atoms in the cation rings (IL ca). Our findings will be compared to the literature data. Specifically, we include previous results for silica melt (SiO₂),^{24,25} the Dzугutov liquid,^{78,79} a 50:50 binary LJ mixture (LJ 50:50),^{11,80} a 80:20 binary LJ mixture (LJ 80:20),^{12–15} a hard sphere (HS) system in a mode-coupling theory (MCT) treatment,⁸¹ and a polymer system featuring finite extensive nonlinear elastic (FENE) springs.⁴³

C. Characterization of spatially heterogeneous dynamics

Previous studies proposed various measures for a characterization of SHD. In general, a coexistence of fast and slow particles results in deviations from a Gaussian distribution of particle displacements. These deviations and, thus, the degree of dynamical heterogeneity, can be quantified based on the non-Gaussian parameter (NGP),

$$\alpha_2(t) = \frac{3 \langle [\mathbf{r}_i(t_0 + t) - \mathbf{r}_i(t_0)]^4 \rangle}{5 \langle [\mathbf{r}_i(t_0 + t) - \mathbf{r}_i(t_0)]^2 \rangle^2} - 1. \quad (3)$$

To characterize both temporal and spatial aspects of heterogeneous dynamics, several approaches focused on clusters of

highly mobile particles.^{6,15,18,24,43,78,82} To construct such clusters, it is custom to select the 5% particles with the highest mobilities, i.e., with the largest displacements in a time interval t , exploiting that, on the relevant time scales, such fraction of particles move substantially farther than expected from Gaussian statistics. Then, a cluster is defined as a group of highly mobile particles that reside in the first neighbor shells of each other. Within this approach, the first minimum of the corresponding intermolecular pair distribution function can be used as a criterion for the extension of the neighbor shell. For a statistical analysis, we determine the probability distribution $p_s(s, t)$ of finding a cluster of size s for a time interval t and calculate the weight-averaged mean cluster size

$$S_w(t) = \frac{\sum_s s^2 p_s(s, t)}{\sum_s s p_s(s, t)}. \quad (4)$$

This quantity measures the average size of a cluster to which a randomly selected highly mobile particle belongs. It was observed that cooperative string-like motion is an important relaxation channel for highly mobile particles.^{15,18,43,78,83,84} Hereby, a string is a group of particles that follow each other along a one-dimensional path. Following these studies, we construct strings by connecting any two particles i and j if the condition

$$\min[|\mathbf{r}_i(t_0) - \mathbf{r}_j(t_0 + t)|, |\mathbf{r}_j(t_0) - \mathbf{r}_i(t_0 + t)|] < \delta \quad (5)$$

holds for the atomic positions at two different times and set δ to about 55% of the respective intermolecular particle distance. This condition describes the situation that one atom has moved away and another atom has filled the vacant position. For an analysis of string-like motion, we determine the probability distribution $p_l(l, t)$ of finding a string of length l in a time interval t and compute the weight-averaged mean string length $L_w(t)$ in analogy with Eq. (4).

Owing to the definitions of strings and clusters, mean cluster sizes $S_w > 1$ and mean string lengths $L_w > 1$ are obtained even if heterogeneous and cooperative dynamics are completely absent. In order to eliminate the random contributions, we discuss the normalized quantities $S_w^*(t) = S_w(t)/S_{rand}$ and $L_w^*(t) = L_w(t)/L_{rand}$. Here, S_{rand} and L_{rand} are the weight-averaged mean values that result when the particles for the cluster and string analyses are randomly selected irrespective of their dynamical behavior.

III. RESULTS

A. Characteristic times of dynamical heterogeneity

To introduce the above measures of the dynamical behavior, we show typical results for dimeric and oligomeric PPO in Fig. 1. For PPO₂, we see a crossover of the MSD from the plateau regime associated with the cage effect in viscous liquids to linear diffusion, providing straightforward access to the self-diffusion coefficient D . Likewise, we observe that the plateau regime of the ISF is followed by a stretched exponential decay, which is caused by the α relaxation and enables a determination of the time constant τ_α . For PPO₉, it is evident that the NGP $\alpha_2(t)$ exhibits a maximum at intermediate times. Similar peaks are found for the mean cluster size $S_w^*(t)$ and the

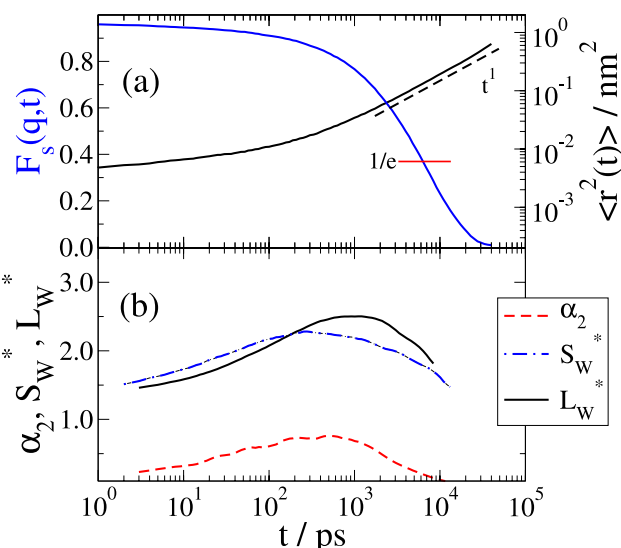


FIG. 1. (a) Mean-square displacement and incoherent scattering function for the oxygen atoms of PPO₂ at 160 K. $F_s(q, t)$ was calculated for a scattering vector of $q = 9.11 \text{ nm}^{-1}$, corresponding to the first maximum of the intermolecular oxygen-oxygen pair distribution function. (b) Non-Gaussian parameter α_2 , mean cluster size S_w^* , and mean string length L_w^* for the oxygen atoms of PPO₉ at 400 K.

mean string length $L_w^*(t)$, albeit the height and the position of the maximum differ for various measures of SHD. For further analysis, we define the maximum values and the maximum positions, i.e., the characteristic times, of these observables according to $\alpha_{2,m} = \alpha_2(\tau_{\alpha_2})$, $S_{w,m}^* = S_w^*(\tau_S)$, and $L_{w,m}^* = L_w^*(\tau_L)$. Upon cooling, the peaks of all these heterogeneity parameters shift to longer times and increase in height, as was reported for various viscous liquids.^{15,18,43,78,84} In the following, we relate these variations to the slowdowns of the structural relaxation and the particle diffusion. In detail, we correlate the characteristic times of the NGP, τ_{α_2} , of the mean cluster size, τ_S , and of the mean string length, τ_L , with the α -relaxation time τ_α in Fig. 2 and with the self-diffusion coefficient D in Fig. 3.

In Fig. 2(a), we see that the time scale of maximum deviation from Gaussian displacement statistics decouples from that of the structural relaxation in a very similar way for various viscous liquids. As indicated by the straight lines, the relation is well described by power laws $\tau_{\alpha_2} \propto \tau_\alpha^{3/4}$. This behavior is found not only for the oligomeric and polymeric systems, cation and anion species of the ionic liquid, and supercooled water of the present work, but also for the LJ mixtures and FENE polymer studied in previous analyses, and even for the paradigm of a strong glass former, SiO₂. In Fig. 2(b), the existence of a common power law for a variety of liquids becomes even clearer based on the scaled time constants $\tau_{\alpha_2}^*$, where the scaling factors were chosen to collapse the data on a single curve. For the Dzугutov liquid, there may be deviations at low temperatures and, hence, long time constants τ_α , but the available data do not allow us to determine whether the effect originates from a high tendency for crystallization in this temperature range.⁸⁵ For the polymers PEO and PBD, the data are consistent with power laws $\tau_{\alpha_2} \propto \tau_\alpha^{3/4}$, definite conclusions are, however, hampered by a notable scattering. Nevertheless, the present approach reveals that, on the one hand, the time scale of maximum dynamical heterogeneity does not directly

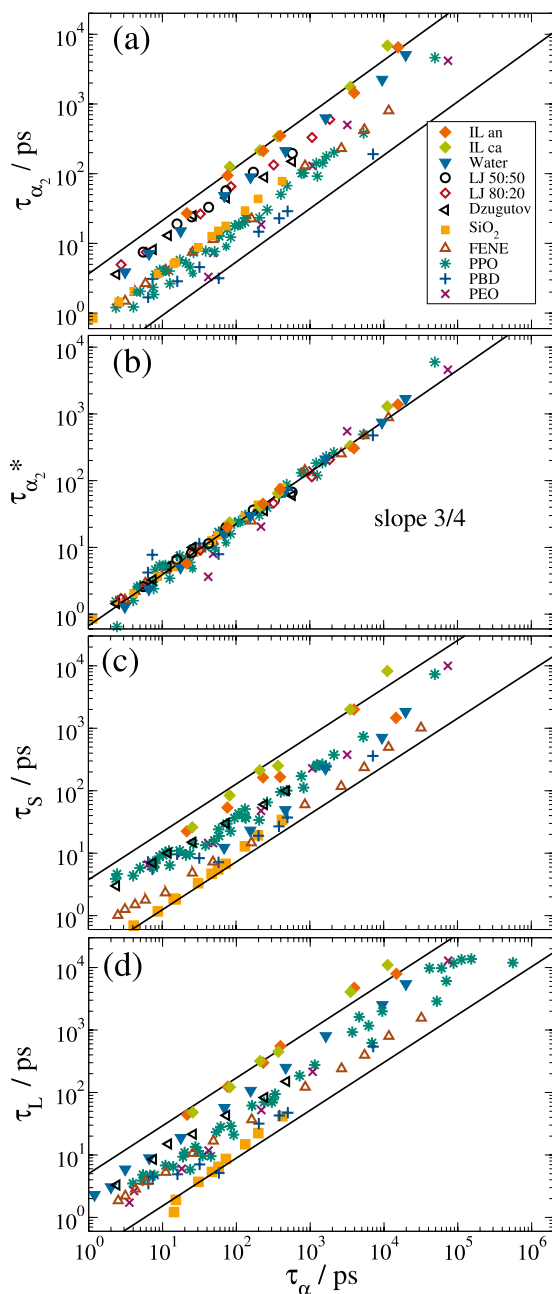


FIG. 2. Characteristic times of maximum dynamical heterogeneity as a function of the corresponding structural relaxation times τ_α . The characteristic times specify the peak positions of the (a) non-Gaussian parameter $\alpha_2(t)$, (c) mean cluster size $S_w^*(t)$, and (d) mean string length $L_w^*(t)$. In panel (b), scaled time constants $\tau_{\alpha_2}^* = \tau_{\alpha_2}/\tau_{\alpha_2,0}$ are shown, where the scaling factors were chosen to obtain best data collapse. Data for supercooled water, an ionic liquid, PEO₁₂, PBD₁₀₀, and PPO with various chain lengths $n = 2$ –100 are shown. The present results are compared with the literature data for SiO₂,^{24,25} 50:50^{11,80} and 80:20^{12–15} LJ mixtures (argon parameter $t = 0.3$ ps),¹¹ the Dzугutov liquid,^{78,79} and a FENE polymer.⁴³ The lines are power laws with an exponent of $\frac{3}{4}$.

follow the slowdown of the α relaxation, while, on the other hand, the decoupling is highly comparable for a broad spectrum of viscous liquids, ranging from atomic to polymeric systems and from fragile to strong glass formers. Moreover, the broad spectrum comprises model liquids, which do and do not feature Coulombic particle interactions, and it includes materials with and without internal degrees of freedom.

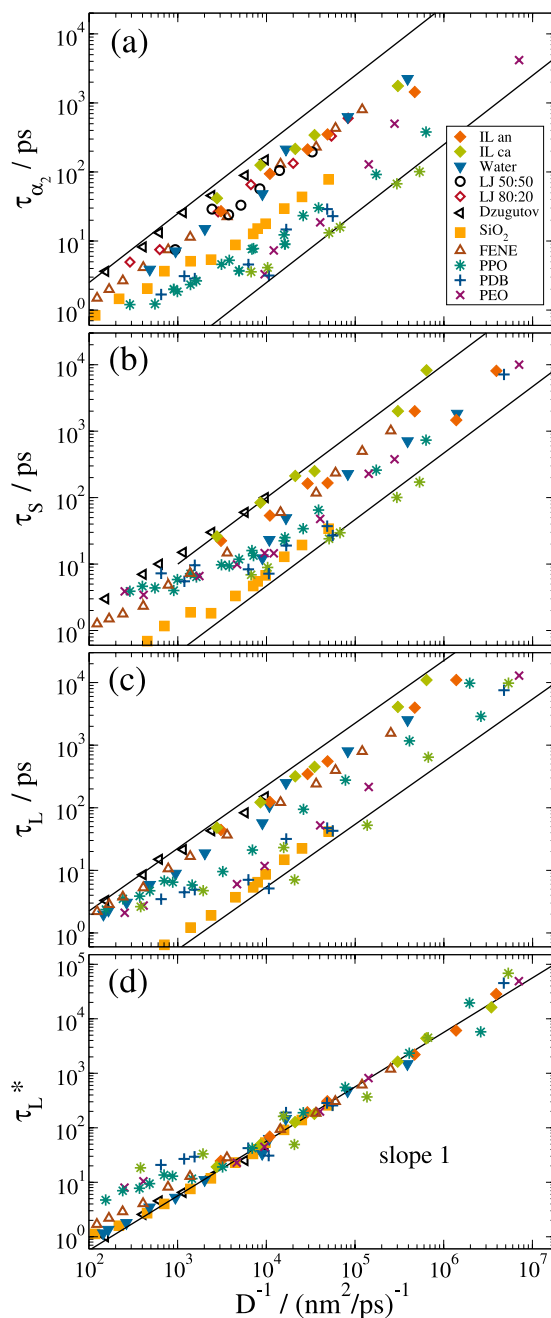


FIG. 3. Characteristic times of maximum dynamical heterogeneity as a function of the corresponding inverse self-diffusion coefficient D^{-1} . The characteristic times specify the peak positions of the (a) non-Gaussian parameter $\alpha_2(t)$, (b) mean cluster size $S_w^*(t)$, and (c) mean string length $L_w^*(t)$. In panel (d), scaled time constants $\tau_L^* = \tau_L/\tau_{L,0}$ are shown, where the scaling factors were chosen to obtain best data collapse. Data for supercooled water, an ionic liquid, PEO₁₂, PBD₁₀₀, and PPO are shown. In the case of PPO, we distinguish between shorter chains $n = 2, 4$ (dark green) and longer chains $n = 18, 36$ (light green). For PPO₄, data at elevated pressure (1–10 kbar) are included. The present results are compared with the literature data for SiO₂,^{24,25} 50:50^{11,80} and 80:20^{12–15} LJ mixtures (argon parameter $t = 0.3$ ps),¹¹ the Dzугutov liquid,^{78,79} and a FENE polymer.⁴³ The lines are linear relations.

In Figs. 2(c) and 2(d), we observe that τ_S and τ_L are also related to τ_α . However, the relation is less uniform among different systems for these measures of maximum SHD than for τ_{α_2} . Specifically, comparison with the straight lines shows that the relations between τ_α and τ_S or τ_L are characterized

by exponents somewhat higher than $\frac{3}{4}$ for silica, water, and the ionic liquid, while the slope is somewhat smaller for the Dzugutov liquid. Therefore, we may conclude that the link to τ_α is weaker for the time scales of maximum cluster size or string length than for that of maximum non-Gaussian behavior.

When $F_s(q, t)$ is analyzed to determine τ_α , the resulting time constant depends on the value of q . For atomic systems, the used values usually correspond to the interparticle distance. For molecular systems, in particular, polymeric systems, it is less obvious which value of q should be chosen. Here, we utilized moduli of the scattering vector which correspond to typical intermolecular distances, e.g., the intermolecular oxygen-oxygen distance in the cases of PEO and PPO. These intermolecular distances and, thus, the probed length scales can be relatively large, resulting in comparatively large values of τ_α . As a consequence of this ambiguous choice of the scattering vector, the characteristic times of different systems can be horizontally shifted with respect to each other when plotted as a function of τ_α . In other words, it is of limited use to discuss the ratio between τ_{α_2} , τ_S , or τ_L and τ_α , as obtained from ISF decays for a specific value of q . However, we determined that when chosen from a reasonable range, the exact value of q does not affect the observed power-law exponent.

Previous work studied clusters of both low-mobility and high-mobility particles for a FENE polymer.⁴³ Observing that the characteristic times of low-mobility clusters exhibit a different temperature dependence than that of high-mobility clusters, including that of string-like motion, it was argued that this difference is at the origin of the SER breakdown. Motivated by these findings, we study whether the present measures of maximum dynamical heterogeneity, in particular, the characteristic times of high-mobility clusters and of string-like motion are related to the self-diffusion coefficient rather than to the α -relaxation time.

In Fig. 3, τ_{α_2} , τ_S , and τ_L are plotted as a function of D^{-1} for several viscous liquids. In Fig. 3(a), we see that the dependence of τ_{α_2} on D^{-1} differs for various systems. The correlation is approximately described by power-laws with different exponents. Linear relations, which are indicated by the straight lines, are the exception rather than the rule. In Fig. 3(b), it can be observed that the situation is similar for the dependence of τ_S on D^{-1} . Smaller differences among the studied systems are found when investigating the correlation between the time scale of maximum string length and the self-diffusion coefficient. In Fig. 3(c), it is evident that as reported for a FENE polymer,⁴³ a linear relation $\tau_L \propto D^{-1}$ approximately describes the data for various systems, ranging from atomic to polymeric systems and from fragile to strong liquids. Furthermore, for PPO₄, the analysis includes results from elevated pressure, $P = 1$ –10 kbar. To further test this relation, we consider the scaled time constants τ_L^* , where the scaling factors are again chosen for best data collapse. In Fig. 3(d), this approach reveals that a linear relation $\tau_L^* \propto D^{-1}$ describes the data for the studied systems for large inverse diffusivities, while there are deviations for, primarily, the polymer melts at small ones, suggesting that vibrational dynamics, in particular, intramolecular contributions, interfere with string motion at high temperatures.

Due to the strong molecular-weight dependence of the self-diffusion coefficient in the case of polymers, the above analyses distinguish between PPO₂ and PPO₄ (dark green stars), on the one hand, and PPO₁₈ and PPO₃₆ (light green stars), on the other. Comparing the results for non-polymeric systems, we find that at a given value of D , the time constants of SHD, particularly, τ_S and τ_L , are significantly shorter for the silica melt than for the atomic and molecular liquids. At present, the origin of this difference is unclear. Also, it remains unanswered why some systems, e.g., the ionic liquid, show $\tau_{\alpha_2} \approx \tau_S \approx \tau_L$, while these time constants differ for others, e.g., water and silica.

B. Breakdown of the Stokes-Einstein relation

The SER links the self-diffusion coefficient D to the shear viscosity η . The proposed linear relation was, however, found to fail for viscous liquids,^{26–44} in particular, fractional relations were reported. Several of these studies exploited the empirical connection between η and τ_α and studied the relation in the form

$$D \propto \left(\frac{\tau_\alpha}{T} \right)^{-\gamma}. \quad (6)$$

Then, an exponent $\gamma = 1$ is expected if the SER is obeyed, while a value $\gamma < 1$ indicates a breakdown of this relation. As aforementioned, such SER breakdown was often rationalized in terms of SHD in combination with the fact that different observables reflect different types of averages over the distributed motional states.⁴⁶ In particular, it was argued that relaxation times and diffusion coefficients result from a time average and a rate average, respectively.

In Fig. 4, we show the dependence of D on τ_α/T for various models of viscous liquids. In the chosen double logarithmic representation, the exponent γ can be directly obtained from the slope of the curves. In the studied temperature ranges, the SER is valid for the SiO₂ and HS systems, while we observe deviations for the other glass formers. For the realistic models of molecular liquids, i.e., the ionic liquid, supercooled water,

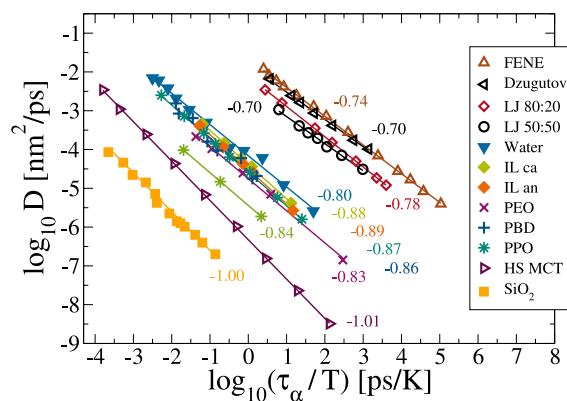


FIG. 4. Self-diffusion coefficient D as a function of τ_α/T for various models of viscous liquids. The present data for an ionic liquid, supercooled water, PEO₁₂, PBD₁₀₀, PPO₂ (dark green), and PPO₂₄ (light green) are compared with the literature data for SiO₂,^{24,25} 50:50^{11,80} and 80:20^{12–15} LJ mixtures, the Dzugutov liquid,^{78,79} a FENE polymer,⁴³ and a HS MCT system.⁸¹ The straight lines are interpolations with Eq. (6). The numbers specify the resulting exponents. The SiO₂ data were shifted downwards by two decades for clarity. In the case of the HS MCT system, $\log_{10} D(\log_{10} \tau_\alpha - 4.5)$ is plotted.

and polymer melts, we find a mild SER breakdown with exponents in the range $\gamma = 0.8$ – 0.9 . For the simpler models, including the FENE polymer, the breakdown is more pronounced, as indicated by smaller exponents $\gamma = 0.7$ – 0.8 . These findings show that SER violations are not limited to the deeply supercooled regime, but they can already occur in the weakly supercooled regime where τ_α is in the pico- or nanoseconds regimes, i.e., above T_c .

C. Relation between the Stokes-Einstein breakdown and spatially heterogeneous dynamics

Next, we ascertain a possible link between the breakdown of the SER and the existence of SHD. If such relation exists, a correlation between the extent of the breakdown and the properties of the heterogeneity may be expected, as proposed in previous works.^{56,57} The above analysis revealed that the fractional exponent γ is an appropriate system-specific measure of deviations from the SER. However, it is less clear which quantity is best suited to quantify the degree of SHD for a given system.

A possible option for the characterization of dynamical heterogeneity is the NGP, e.g., its peak value $\alpha_{2,m} = \alpha_2(\tau_{\alpha_2})$. In view of the strong temperature dependence of this quantity, it is, however, essential to consider corresponding state points when intending to compare results for various systems. Here, we choose state points with identical self-diffusion coefficients. In Fig. 5, the dependence of the peak height $\alpha_{2,m}$ on the diffusion coefficient D is shown for several viscous liquids. We see that the value of $\alpha_{2,m}$ at any given value D is not correlated with the degree of deviations from the SER. Specifically, viscous liquids, which show no or mild SER breakdowns, e.g., silica and water, exhibit high values of $\alpha_{2,m}$, while small values of $\alpha_{2,m}$ are found for polymer melts with a pronounced SER breakdown. Thus, our analysis does not yield evidence for a relation between the peak height of the NGP and the failure of the SER. Likewise, the maximum cluster and string sizes are not correlated to the degree of the decoupling of structural relaxation and self-diffusion (not shown). As a consequence of the construction of the clusters and strings, which involves the search for neighboring

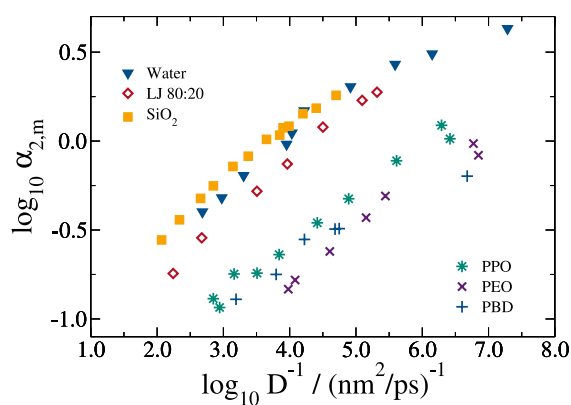


FIG. 5. Peak value of the non-Gaussian parameter, $\alpha_{2,m}$, as a function of the inverse self-diffusion coefficient D^{-1} . The present data for supercooled water, PEO₁₂, PBD₁₀₀, and PPO₂ are compared with the literature data for SiO₂^{24,25} and a 80:20 LJ mixture.^{12–15}

particles with appropriate dynamical behavior, the sizes of these entities strongly depend on the coordination numbers, hampering meaningful comparisons of different systems and rationalizing missing correlations. In future studies, the latter problem may be overcome based on the four-point dynamic susceptibility χ_4 , which was recently found to be related to the SER breakdown.⁵⁶ Presently, the available data base does, however, not suffice to establish robust links between χ_4 and τ_α or D^{-1} across a broad spectrum of liquids spanning from atomic to polymeric systems.

Another possible measure of dynamical heterogeneity is the nonexponentiality of correlation functions, as broad mobility distributions are expected to result in a more gradual decrease. Following this idea, we determine the nonexponentiality of the α relaxation by fitting the corresponding decay of $F_s(q, t)$ to a stretched exponential

$$F_s(q, t) \propto \exp \left[- \left(\frac{t}{\tau} \right)^\beta \right] \quad (0 \leq \beta \leq 1). \quad (7)$$

Then, the value of the stretching parameter β specifies the deviation from exponential behavior. Previously, we observed that β decreases towards a plateau value upon cooling.¹⁹ Thus, this plateau value can be regarded as a system-specific measure of the nonexponentiality. In Fig. 6, we study the relation between γ and β for various viscous liquids. We see that systems with higher β values, i.e., weaker stretching, tend to show higher γ values, i.e., weaker deviations from the SER relation. These results imply a correlation between the degree of SHD and the extent of the decoupling between relaxation times and diffusion coefficients. We note that in order to ensure consistent fitting procedures, the β values for the LJ and HS systems were obtained by refitting the literature data from Refs. 80, 81, and 86.

One may argue that the chosen approach suffers from the fact that $F_s(q, t)$ is characterized by different time constants and stretching parameters when the value of q is modified and, hence, dynamics on various length scales is probed. While a change of the time constant may influence the value of γ , a variation of the stretching parameter results from the effect that

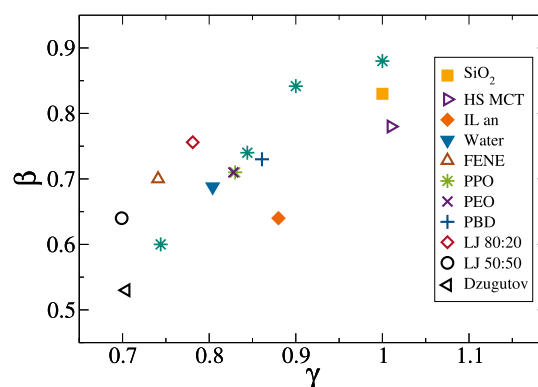


FIG. 6. Relation between the stretching parameter β of the α relaxation, see Eq. (7), and the exponent parameter γ , of the fractional SER, see Eq. (6). The present data for an ionic liquid, supercooled water, PEO₁₂, PBD₁₀₀, and PPO₂₄ (light green star) are compared with the literature data for SiO₂,²⁵ 50:50^{11,80} and 80:20^{12–15} LJ mixtures, the Dzgutov liquid,^{78,79} a HS MCT system,⁸¹ and a FENE polymer.⁴³ For PPO₂ (dark green stars), we compare results obtained from analyses of $F_s(q, t)$ for q values of 3.9, 7.1, 12, and 24 nm⁻¹.

averaging over spatial inhomogeneity is more efficient at larger length and time scales, leading to reduced nonexponentiality. To determine the relevance of these effects for the example of PPO₂, we compare results for q values of 3.9, 7.1, 12, and 24 nm⁻¹ in Fig. 6. We find that when decreasing q , both β and γ increase. Hereby, the q -dependent data for PPO₂ follow the relation $\beta(\gamma)$ obtained from the above comparison of different systems. This finding shows that the choice of q is not critical for the present analysis.

IV. CONCLUSIONS

Performing MD simulations for various types of viscous liquids, we ascertained relations between dynamical heterogeneity, α relaxation, and self-diffusion. In order to characterize the space-time characteristics of dynamical heterogeneity, the degree of deviations from Gaussian displacement statistics, the size of high-mobility clusters, and the length of cooperatively-rearranging strings were determined. On the one hand, the characteristic times of maximum non-Gaussian parameter (τ_{α_2}), cluster size (τ_S), and string length (τ_L) decouple from that of the structural relaxation upon cooling for all studied systems. While the degree of the decoupling varies among different systems for the cluster and string characteristics, a largely universal relation was found for the non-Gaussian parameter, $\tau_{\alpha_2} \propto \tau_{\alpha}^{3/4}$. The spectrum of viscous liquids showing such remarkable uniformity ranges from atomic to polymeric systems and from fragile to strong glass formers and it comprises model liquids, which do and do not feature Coulombic particle interactions. Hence, the observed power-law decoupling between non-Gaussianity and α relaxation appears to be a generic feature of glass-forming liquids, at least in the regime of moderate viscosity accessible to simulation studies. On the other hand, the characteristic times of dynamical heterogeneity do not necessarily decouple from the inverse self-diffusion coefficient. While the relation between τ_{α_2} or τ_S and D^{-1} is not uniform among the studied systems, linear behavior was found for the time scale of maximum string length, $\tau_L \propto D^{-1}$. More precisely, such linear relation was found at low temperatures, while there can be deviations at high temperatures, where structural relaxation and vibrational motion are not well separated. Thus, the present analysis puts previous results⁴³ for the connection of string motion and self-diffusion on a broader data base. In that study,⁴³ it was argued that the particles showing string motion are a major fraction of the particles exhibiting high mobility, which in turn dominate the diffusion coefficient and that these strings are good candidates for the cooperatively rearranging regions of the Adam-Gibbs theory.

A possible decoupling of structural relaxation and self-diffusion was ascertained based on the fractional Stokes-Einstein exponent γ . While the Stokes-Einstein relation holds for a hard-sphere system and silica melt ($\gamma = 1$), it clearly fails for molecular liquids, including polymer melts, and, in particular, atomic glass formers. We investigated to what extent a Stokes-Einstein breakdown is brought about by the existence of dynamical heterogeneity. We observed no straightforward correlation between the degree of deviation from the Stokes-Einstein prediction and the peak height of the non-Gaussian

parameter or the maximum cluster and string sizes. However, we found smaller fractional exponents γ , i.e., more prominent breakdowns, for systems with smaller stretching parameters β and, thus, more nonexponential α relaxation. All these effects are not limited to the deeply supercooled regime at low temperatures or high pressures, but they already occur in the moderately supercooled regime $T > T_c$. As the four-point dynamic susceptibility χ_4 probes SHD on longer time scales than the quantities considered in the present study, it may be worthwhile to further ascertain the relation between the properties of this generalized susceptibility and the relaxation and diffusion behavior of viscous liquids in future work.

ACKNOWLEDGMENTS

The authors thank the Deutsche Forschungsgemeinschaft (DFG) for funding through Project Nos. VO 905/5-1 and VO 905/9-2 as well as through the Collaborative Research Center/Transregio TRR 146 (Project A6).

- ¹C. A. Angell, K. L. Ngai, G. B. McKenna, P. F. McMillan, and S. W. Martin, *J. Appl. Phys.* **88**, 3113 (2000).
- ²C. M. Roland, S. Hensel-Bielowka, M. Paluch, and R. Casalini, *Rep. Prog. Phys.* **68**, 1405 (2005).
- ³L. Berthier and G. Biroli, *Rev. Mod. Phys.* **83**, 587 (2011).
- ⁴P. G. Debenedetti and F. H. Stillinger, *Nature* **410**, 259 (2001).
- ⁵K. Binder, *J. Non-Cryst. Solids* **274**, 332 (2000).
- ⁶S. C. Glotzer, *J. Non-Cryst. Solids* **274**, 342 (2000).
- ⁷W. Kob, M. Nauroth, and F. Sciortino, *J. Non-Cryst. Solids* **307-310**, 181 (2002).
- ⁸W. Paul and G. D. Smith, *Rep. Prog. Phys.* **67**, 1117 (2004).
- ⁹J. Baschnagel and F. Varnik, *J. Phys.: Condens. Matter* **17**, R851 (2005).
- ¹⁰A. Heuer, *J. Phys.: Condens. Matter* **20**, 373101 (2008).
- ¹¹S. C. Glotzer, V. N. Novikov, and T. B. Schröder, *J. Chem. Phys.* **112**, 509 (2000).
- ¹²W. Kob and H. C. Andersen, *Phys. Rev. E* **51**, 4626 (1995).
- ¹³W. Kob, C. Donati, S. J. Plimpton, P. H. Poole, and S. C. Glotzer, *Phys. Rev. Lett.* **79**, 2827 (1997).
- ¹⁴K. Vollmayr-Lee, W. Kob, K. Binder, and A. Zippelius, *J. Chem. Phys.* **116**, 5158 (2002).
- ¹⁵C. Donati, S. C. Glotzer, P. H. Poole, W. Kob, and S. J. Plimpton, *Phys. Rev. E* **60**, 3107 (1999).
- ¹⁶C. Donati, S. C. Glotzer, and P. H. Poole, *Phys. Rev. Lett.* **82**, 5064 (1999).
- ¹⁷C. Bennemann, C. Donati, J. Baschnagel, and S. C. Glotzer, *Nature* **399**, 246 (1999).
- ¹⁸M. Vogel, *Macromolecules* **41**, 2949 (2008).
- ¹⁹A. Bormuth, P. Henritzi, and M. Vogel, *Macromolecules* **43**, 8985 (2010).
- ²⁰R. Böhmer, R. Chamberlin, G. Diezemann, B. Geil, A. Heuer, G. Hinze, S. Kuebler, R. Richert, B. Schiener, H. Sillescu et al., *J. Non-Cryst. Solids* **235**, 1 (1998).
- ²¹H. Sillescu, *J. Non-Cryst. Solids* **243**, 81 (1999).
- ²²M. Ediger, *Annu. Rev. Phys. Chem.* **51**, 99 (2000).
- ²³R. Richert, *J. Phys.: Condens. Matter* **14**, R703 (2002).
- ²⁴M. Vogel and S. C. Glotzer, *Phys. Rev. Lett.* **92**, 255901 (2004).
- ²⁵M. Vogel and S. C. Glotzer, *Phys. Rev. E* **70**, 061504 (2004).
- ²⁶S. R. Becker, P. H. Poole, and F. W. Starr, *Phys. Rev. Lett.* **97**, 055901 (2006).
- ²⁷L. Xu, F. Mallamace, Z. Yan, F. W. Starr, S. V. Buldyrev, and H. E. Stanley, *Nat. Phys.* **5**, 565 (2009).
- ²⁸A. Turberfield, S. Haynes, P. Wright, R. Ford, R. Clark, J. Ryan, J. Harris, and C. Foxon, *Phys. Rev. Lett.* **65**, 637 (1990).
- ²⁹E. Rössler, *Phys. Rev. Lett.* **65**, 1595 (1990).
- ³⁰I. Chang, F. Fujara, B. Geil, G. Heuberger, T. Mangel, and H. Sillescu, *J. Non-Cryst. Solids* **172 - 174**, 248 (1994).
- ³¹M. T. Cicerone and M. Ediger, *J. Chem. Phys.* **104**, 7210 (1996).
- ³²S. F. Swallen, P. A. Bonvallet, R. J. McMahon, and M. D. Ediger, *Phys. Rev. Lett.* **90**, 015901 (2003).
- ³³M. K. Mapes, S. F. Swallen, and M. D. Ediger, *J. Phys. Chem. B* **110**, 507 (2006).
- ³⁴F. Mallamace, C. Branca, C. Corsaro, N. Leone, J. Spooren, H. E. Stanley, and S.-H. Chen, *J. Phys. Chem. B* **114**, 1870 (2010).

- ³⁵F. Fernandez-Alonso, F. Bermejo, S. McLain, J. Turner, J. Molaison, and K. Herwig, *Phys. Rev. Lett.* **98**, 077801 (2007).
- ³⁶L. Berthier, *Phys. Rev. E* **69**, 020201 (2004).
- ³⁷T. G. Lombardo, P. G. Debenedetti, and F. H. Stillinger, *J. Chem. Phys.* **125**, 174507 (2006).
- ³⁸M. G. Mazza, N. Giovambattista, H. E. Stanley, and F. W. Starr, *Phys. Rev. E* **76**, 031203 (2007).
- ³⁹S. K. Kumar, G. Szamel, and J. F. Douglas, *J. Chem. Phys.* **124**, 214501 (2006).
- ⁴⁰F. Affouard, M. Descamps, L.-C. Valdes, J. Habasaki, P. Bordat, and K. L. Ngai, *J. Chem. Phys.* **131**, 104510 (2009).
- ⁴¹A. Ikeda and K. Miyazaki, *Phys. Rev. Lett.* **106**, 015701 (2011).
- ⁴²S. Sengupta, S. Karmakar, C. Dasgupta, and S. Sastry, *J. Chem. Phys.* **138**, 12A548 (2013).
- ⁴³F. W. Starr, J. F. Douglas, and S. Sastry, *J. Chem. Phys.* **138**, 12A541 (2013).
- ⁴⁴T. Kawasaki and A. Onuki, *Phys. Rev. E* **87**, 012312 (2013).
- ⁴⁵J. A. Hodgdon and F. H. Stillinger, *Phys. Rev. E* **48**, 207 (1993).
- ⁴⁶G. Tarjus and D. Kivelson, *J. Chem. Phys.* **103**, 3071 (1995).
- ⁴⁷Y. J. Jung, J. P. Garrahan, and D. Chandler, *Phys. Rev. E* **69**, 061205 (2004).
- ⁴⁸A. C. Pan, J. P. Garrahan, and D. Chandler, *Phys. Rev. E* **72**, 041106 (2005).
- ⁴⁹X. Xia and P. G. Wolynes, *J. Phys. Chem. B* **105**, 6570 (2001).
- ⁵⁰G. Biroli and J.-P. Bouchaud, *J. Phys.: Condens. Matter* **19**, 205101 (2007).
- ⁵¹S.-H. Chong, *Phys. Rev. E* **78**, 041501 (2008).
- ⁵²E. J. Saltzman and K. S. Schweizer, *Phys. Rev. E* **77**, 051505 (2008).
- ⁵³G. Diezemann, H. Sillescu, G. Hinze, and R. Böhmer, *Phys. Rev. E* **57**, 4398 (1998).
- ⁵⁴K. L. Ngai, *J. Phys. Chem. B* **103**, 10684 (1999).
- ⁵⁵R. Zangi and L. J. Kaufman, *Phys. Rev. E* **75**, 051501 (2007).
- ⁵⁶E. Flenner, H. Staley, and G. Szamel, *Phys. Rev. Lett.* **112**, 097801 (2014).
- ⁵⁷C. K. Mishra and R. Ganapathy, *Phys. Rev. Lett.* **114**, 198302 (2015).
- ⁵⁸O. Borodin and G. D. Smith, *J. Phys. Chem. B* **107**, 6801 (2003).
- ⁵⁹G. D. Smith, O. Borodin, and D. Bedrov, *J. Phys. Chem. A* **102**, 10318 (1998).
- ⁶⁰P. Henritzi, A. Bormuth, and M. Vogel, *Solid State Nucl. Magn. Reson.* **54**, 32 (2013).
- ⁶¹G. D. Smith and W. Paul, *Macromolecules* **32**, 8857 (1999).
- ⁶²F. Klameth and M. Vogel, *J. Chem. Phys.* **138**, 134503 (2013).
- ⁶³F. Klameth, P. Henritzi, and M. Vogel, *J. Chem. Phys.* **140**, 144501 (2014).
- ⁶⁴H. Berendsen, J. Grigera, and T. Straatsma, *J. Phys. Chem.* **91**, 6269 (1987).
- ⁶⁵W. Zhao, F. Leroy, S. Balasubramanian, and F. Müller-Plathe, *J. Phys. Chem. B* **112**, 8129 (2008).
- ⁶⁶J. N. Canongia Lopes, J. Deschamps, and A. A. Pádua, *J. Phys. Chem. B* **108**, 2038 (2004).
- ⁶⁷O. Borodin, G. D. Smith, and R. L. Jaffe, *J. Comput. Chem.* **22**, 641 (2001).
- ⁶⁸H. J. Berendsen, D. van der Spoel, and R. van Drunen, *Comput. Phys. Commun.* **91**, 43 (1995).
- ⁶⁹B. Hess, H. Bekker, H. J. Berendsen, and J. G. Fraaije, *J. Comput. Chem.* **18**, 1463 (1997).
- ⁷⁰E. Lindahl, B. Hess, and D. Van Der Spoel, *J. Mol. Model.* **7**, 306 (2001).
- ⁷¹D. Van Der Spoel, E. Lindahl, B. Hess, G. Groenhof, A. E. Mark, and H. J. Berendsen, *J. Comput. Chem.* **26**, 1701 (2005).
- ⁷²B. Hess, C. Kutzner, D. van der Spoel, and E. Lindahl, *J. Chem. Theory Comput.* **4**, 435 (2008).
- ⁷³T. Darden, D. York, and L. Pederson, *J. Chem. Phys.* **98**, 10089 (1993).
- ⁷⁴S. Nosé, *J. Chem. Phys.* **81**, 511 (1984).
- ⁷⁵W. G. Hoover, *Phys. Rev. A* **31**, 1695 (1985).
- ⁷⁶M. Parrinello and A. Rahman, *J. Appl. Phys.* **52**, 7182 (1981).
- ⁷⁷A. Bormuth, M. Hofmann, P. Henritzi, M. Vogel, and E. A. Rössler, *Macromolecules* **46**, 7805 (2013).
- ⁷⁸Y. Gebremichael, M. Vogel, and S. C. Glotzer, *J. Chem. Phys.* **120**, 4415 (2004).
- ⁷⁹Y. Gebremichael, Ph.D. thesis, University of Maryland, College Park, MD, 2004, <http://hdl.handle.net/1903/236>.
- ⁸⁰T. B. Schröder, Ph.D. thesis, Roskilde University, Denmark, 2000; e-print [arXiv:cond-mat/0005127](https://arxiv.org/abs/cond-mat/0005127).
- ⁸¹M. Fuchs, W. Götze, and M. R. Mayr, *Phys. Rev. E* **58**, 3384 (1998).
- ⁸²N. Giovambattista, S. V. Buldyrev, F. W. Starr, and H. E. Stanley, *Phys. Rev. Lett.* **90**, 085506 (2003).
- ⁸³C. Donati, J. F. Douglas, W. Kob, S. J. Plimpton, P. H. Poole, and S. C. Glotzer, *Phys. Rev. Lett.* **80**, 2338 (1998).
- ⁸⁴M. Aichele, Y. Gebremichael, F. W. Starr, J. Baschnagel, and S. C. Glotzer, *J. Chem. Phys.* **119**, 5290 (2003).
- ⁸⁵Y. Gebremichael, M. Vogel, M. N. J. Bergroth, F. W. Starr, and S. C. Glotzer, *J. Phys. Chem. B* **109**, 15068 (2005).
- ⁸⁶W. Kob and H. C. Andersen, *Phys. Rev. Lett.* **73**, 1376 (1994).